A Bioactive Carbon Nanotube-Based Ink for Printing 2D and 3D Flexible Electronics

*Su Ryon Shin, Raziyeh Farzad, Ali Tamayol, Vijayan Manoharan, Pooria Mostafalu, Yu Shrike Zhang, Mohsen Akbari, Sung Mi Jung, Duckjin Kim, Mattia Comotto, Nasim Annabi, Faten Ebrahim Al-Hazmi, Mehmet R. Dokmeci, and Ali Khademhosseini**

Flexible and stretchable electronics have generated significant interest for various biomedical applications such as epidermal sensors, smart sutures, soft contact lenses, artificial electronic muscles, neuron-to-machine interfaces, implantable medical devices, and artificial skin.[1] In all of these applications, the proper function of the platform relies on its reliable electrical performance under various loading conditions and deformations. For example, with respect to electronic devices that interface with tissues, such as electrocardiogram mapping devices or minimally invasive surgical tools, it is desirable to have properties such as stretchability, foldability, bendability, and biocompatibility so that devices can adapt to tissue and body motions while maintaining intimate and conformal contact.[2–4]

Dr. S. R. Shin, R. Farzad, Dr. A. Tamayol, V. Manoharan, Dr. P. Mostafalu, Dr. Y. S. Zhang, Dr. M. Akbari, Dr. D. Kim, M. Comotto, Prof. N. Annabi, Dr. M. R. Dokmeci, Prof. A. Khademhosseini
Biomaterials Innovation Research Center
Department of Medicine
Brigham and Women's Hospital
Harvard Medical School
Boston, MA 02139, USA
E-mail: alik@rics.bwh.harvard.edu

Dr. S. R. Shin, R. Farzad, Dr. A. Tamayol, V. Manoharan, Dr. P. Mostafalu, Dr. Y. S. Zhang, Dr. M. Akbari, Dr. D. Kim, M. Comotto, Prof. N. Annabi, Dr. M. R. Dokmeci, Prof. A. Khademhosseini
Harvard-MIT Division of Health Sciences and Technology
Massachusetts Institute of Technology
Cambridge, MA 02139, USA

Dr. S. R. Shin, Dr. A. Tamayol, Dr. P. Mostafalu, Dr. Y. S. Zhang, Dr. M. Akbari, Prof. N. Annabi, Dr. M. R. Dokmeci, Prof. A. Khademhosseini
Wyss Institute for Biologically Inspired Engineering
Harvard University
Boston, MA 02115, USA

Dr. S. M. Jung
Department of Electrical Engineering and Computer Science
Massachusetts Institute of Technology
Cambridge, MA 02139, USA

Prof. N. Annabi
Department of Chemical Engineering
Northeastern University
Boston, MA 02115-5000, USA

Dr. F. E. Al-Hazmi, Prof. A. Khademhosseini
Department of Physics and Department of Chemistry
Faculty of Science
King Abdulaziz University
Jeddah 21589, Saudi Arabia

DOI: 10.1002/adma.201506420

Currently, most flexible electronic devices are made by using serpentine and wavy conductive patterns, either freestanding or formed on flexible and elastic substrates.[4–6] The free-standing metallic lines can maintain conformal contact to curved surfaces and do not restrict the movement of the surface after contact. However, they are susceptible to mechanical failure due to the lack of a load-bearing supportive substrate and also usually require complex microfabrication technologies.[5] The utilization of flexible substrates can increase the mechanical robustness of the engineered electronic devices, simplify the fabrication process, and extend their functionality toward various applications such as advanced drug delivery platforms.[7] The strategies for fabrication of conductive patterns on flexible substrates include the use of printable conductive inks and the deposition process that utilize different techniques such as screen printing, contact printing, and transfer printing.[8,9] Among these technologies, printing conductive inks has drawn significant attention for fabrication of complex 2D or 3D flexible electronics owing to its robustness, cost effectiveness, and the high resolution of emerging commercial printers.[10,11] In contrast to other microfabrication technologies that mostly result in planar structures, printing allows the fabrication of complex electrical circuits in a 3D manner.[12,13]

The conductive inks currently employed in printing processes are usually based on volatile solutions containing conducting or semi-conducting micro- and nanoscale materials in the form of metallic nanorods, conducting polymer nanoparticles, carbon nanotubes (CNTs), graphene, or a mixture of these materials.[3,12] Particularly, CNT-based inks have emerged as a promising candidate for the fabrication of flexible electronics using printing technique owing to their excellent mechanical and electrical properties, especially their electrical conductivity.[5,14,15] Furthermore, the versatility of CNTs has enabled the fabrication of different devices such as flexible actuators, supercapacitors, sensors, and transistors using printing techniques. Several CNT-based conductive inks have been developed over the past years.[16] These inks are either cytotoxic or lack biological cues to induce desired cellular behavior. Moreover, those inks usually contained volatile organic solvents and toxic materials that are prone to generating defects in the substrate. Thus, there is a need for the development of bioactive and conductive inks for engineering 2D and 3D constructs. In this study, we have developed conductive inks that can be used for fabrication of 2D constructs. We then modified the ink in a way that allows creating 3D structures using a bioprinting approach. Proposed inks possess cell-binding sites allowing facile interfacing with living tissues and organisms.

To address these limitations, we used deoxyribonucleic acid (DNA) as a natural surfactant to disperse CNTs in various biomaterials such as gelatin methacryloyl (GelMA) and hyaluronic acid (HA) to form bioactive CNT-based hybrid inks. These biomaterials can be used as binders to enhance CNT–CNT and CNT–substrate interactions.[17,18] The physical properties of the engineered conductive ink can be tuned by changing composition of the biomaterials and type of CNTs to enable 2D and 3D printing of flexible constructs and circuits. In addition, the bioinks have shown excellent cellular biocompatibility and bioactivity. Therefore, we expect a good biocompatibility for the generated biomaterial/CNT hybrid inks as well as enhanced electrical and mechanical properties, which makes them suitable candidates for various biological and biomedical applications.[19] Furthermore, due to their low processing temperatures during deposition, the synthesized hybrid inks can be used to fabricate devices on flexible polymeric substrates, which are not compatible with fabrication techniques including the high-temperature deposition processes.[20]

To create flexible and durable 2D electrodes with cell-adhesive properties, GelMA was utilized, whereas for generating 3D electrodes HA was used. GelMA is derived from gelatin, which is denatured from collagen, a biocompatible material with cell binding sequences.[21] Gelatin has a random coil structure in solution, which can partially form α-helix structures below 23 °C.[22] Therefore, the unique structural, physicomechanical, and biological properties of gelatin or its chemical derivatives in aqueous environment can improve particle–particle or particle–substrate interactions with proper bioactivity. To increase the stability of 2D electrodes within biological solutions, gelatin can be modified via methacrylation, which can be cross-linked using UV light. In addition, GelMA has been previously used in coating nanomaterials which enabled homogeneous dispersions of carboxyl-functionalized multiwalled carbon nanotubes (MWCNTs) in a biological medium.[17]

The use of high GelMA concentrations (>20 mg mL^{-1}) for dispersion of MWCNTs can lead to an increase in the electrical resistance between CNT–CNT junctions and affect particle dispersion.[23] This could be more detrimental especially for developing an electrically conductive ink, where a high concentration of nonfunctionalized MWCNTs is required (≈6 mg mL^{-1}).[18] For this reason, DNA is used as a biosurfactant to facilitate CNT dispersion within the aqueous solution. DNA segments have many bases, which can strongly bind to the surface of CNTs due to the π–π stacking interactions. Also, a large number of phosphate groups of DNA segments can interact with water, improving the dispersion of CNTs at high concentrations compared to other cytotoxic surfactants.[24,25] For example, CNTs were coated with DNA to improve their solubility while preserving their electrical conductivity which are used as actuator and supercapacitor.[26–28] In our work, the DNA segments were disturbed during the sonication process and subsequently reoriented and covered the surface of individual MWCNTs through π–π stacking interactions, hydrogen bonding, and hydrophobic interactions.[24] Furthermore, the use of GelMA improved the particle separation and prevented aggregate formation reported in our previous study.[17] Therefore, the GelMA/DNA combination is an ideal mixture of natural materials which can be used as biocompatible binders for nanoparticles to enhance the tolerance to strain and folding while preserving proper bioactivity and high electrical conductivity (**Figure 1**a). The use of GelMA/DNA (3 mg mL^{-1} GelMA, 4 mg mL^{-1} DNA) enabled us to successfully disperse high concentrations of MWCNTs (6 mg mL^{-1}) in aqueous solutions and to obtain a black-ink solution (Figure 1b, photograph). The transmission electron microscopy (TEM) image shows the well-dispersed MWCNT networks after being coated with GelMA/DNA, confirming the presence of a thin GelMA/DNA layer on the surface of the nanotubes (Figure 1b). We analyzed the bare MWCNTs and GelMA/DNA-coated MWCNTs with Raman spectroscopy to confirm the absence of defects on MWCNTs during the coating process that involved sonication. The ratio between the two characteristic peaks of CNTs at 1300 cm^{-1} (D-band) and 1592 cm^{-1} (G-band) is commonly used as an indicator of the structural defects.[18] The ratio of G- to D-band in both MWCNTs was found to be similar, suggesting that there was no distinction in the spectra between the pristine CNTs (I_G/I_D: 1.67) and GelMA/DNA-coated MWCNTs (I_G/I_D: 1.66) (Figure 1c). Therefore, it is expected that the high viscosity of the DNA (4 mg mL^{-1}, 185 Pa s at 0.01 s^{-1}) solution preserved the structural integrity of nanotubes during the relatively short dispersion process (≈2 h) (Figure S1, Supporting Information).[29]

The developed ink was used to create free-standing hybrid films (thickness ≈10 µm) by coating a thin layer on a glass substrate followed by peeling it off after drying. The hybrid film was flexible and resilient against bending and rolling (Figure 1d). We confirmed that GelMA/DNA-coated MWCNTs could generate a network due to Van der Waals interactions between nanotubes. Scanning electron microscopy (SEM) images of a cross-section of the film showed a well-resolved network of GelMA/DNA-coated MWCNTs (Figure 1d). The electrical conductivity of the dried hybrid film was 24 ± 1.8 S cm^{-1} as measured by a four-point probe method.[27] Even after drying (films containing ≈47% GelMA/DNA, which was confirmed by thermogravimetric analysis (Figure S2, Supporting Information), the conductivity of these films was higher than 2D-printed graphene patterns (0.1–100 S m^{-1}).[9,11,30] This is due to the fact that the unique electrical property of the double strand DNA could decrease the junction resistance between CNTs at junction points compared to other polymer binders, which can be due to strong π–π interactions between the DNA and CNT walls.[28,31] The electrical conductivity of the films was demonstrated by printing a circuit onto a cellulose paper and turning on a light-emitting diode (LED) by applying a 1.5 V potential (Figure S3, Supporting Information).

The engineered electrically conductive ink was compatible with different fabrication processes such as extrusion based printing, screen printing, and dip-coating. Using these microfabrication techniques, inks were deposited on a variety of substrates including cellulose paper, polyethylene glycol (PEG) coated polyethylene terephthalate (PET) flexible films, highly swellable hydrogel sheets, electrospun sheets, elastic alginate-based hydrocolloid substrates used as wet wound dressings, and cotton thread (Figure 1f–h). The GelMA/DNA-coated MWCNT ink showed viscosity of ≈0.01 Pa s at 50 s^{-1} shear rate which is related to our bioprinting process (Figure 1e), and it is lower than previous reports utilizing extrusion based printing

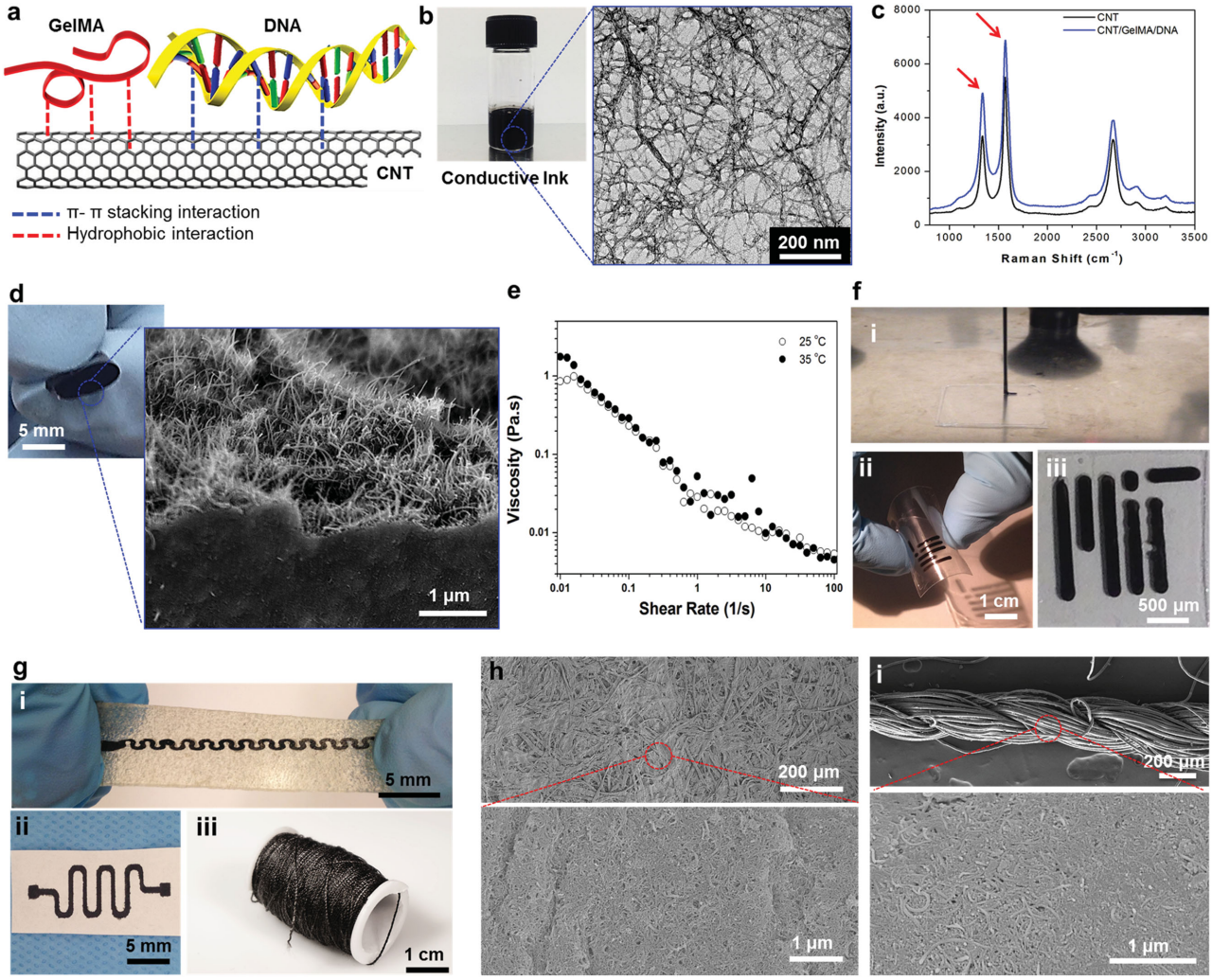

Figure 1. Formation and characterization of the electrically conductive ink and its utilization. a) Schematic diagram showing the GelMA/DNA-coated MWCNT inks formed though hydrogen bonding, hydrophobic interactions, and π–π stacking interactions between MWCNT and GelMA/DNA. b) Photograph of black conductive ink and high-resolution TEM image of individual or bundled GelMA/DNA-wrapped MWCNTs. c) Raman spectrum of the MWCNTs and GelMA/DNA-coated MWCNTs. d) Representative images of highly flexible hybrid films after rolling and a magnified SEM image showing a cross-section of MWCNTs coated with GelMA/DNA. e) Viscosity dependence as a function of shear rate for GelMA/DNA-coated MWCNT inks. f) Photograph of (i) nozzle-based printing using a glass capillary (ii) on a PEG-coated PET film, and (iii) cellulose paper substrate. g) Screen printing on (i) stretchable hydrocolloid substrate and (ii) cellulose paper (iii) dip-coating on cotton thread. h) SEM image of screen-printed cellulose paper by GelMA/DNA-coated MWCNT ink. i) SEM image of uniformly covered GelMA/DNA-coated MWCNT ink on a cotton thread.

methodologies with graphene-based inks (10–50 Pa s at 10 s^{-1})[32] and carbon filler incorporated inks (≈20 Pa s at 50 s^{-1}).[33] These characteristics are key requirements for the ink to prevent nozzles from clogging during the printing process.[34] The direct write printer was used to automatically produce various predefined patterns by moderating the flow rates (23.6 μL min^{-1}) and the nozzle movement speeds (120 mm min^{-1}) (Figure 1f (i)). Figure 1f (ii and iii) shows a MIT logo printed on a PEG-coated PET film. In addition, using screen printing, various patterns were fabricated on a stretchable hydrocolloid substrate (Figure 1g (i)) and cellulose paper (Figure 1g (ii)). Magnified SEM images of the surface of a microfibrous cellulose paper showed a GelMA/DNA-coated MWCNTs network (Figure 1h). The strong adhesion of the electrically conductive ink to the substrate facilitated the screen printing process and resulted in the fabrication of complex patterns with higher resolution (linewidths as small as 100 μm), which are comparable to what other groups have achieved.[9,12,35] This resolution is better than what is achievable with commercially available conductive silver inks. Another advantage of using developed electrically conductive ink which is made up of an aqueous solvent is that the printing process results in reduced substrate damage compared to the link that consist of organic solvents (acetone, isopropanol, ethanol, dichloromethane, etc.) used in the majority of commercially available electrically conductive inks.[12,19]

CNT-based conductive yarns have also been employed for the fabrication of wearable electronics.[36] Textile processing is an emerging process which is low-cost, easy to use, and adaptable to many manufacturing processes.[37] Here, we utilized the coating technology developed by our group to coat cotton

threads with the electrically conductive inks.[37] The homogeneity of the developed ink enabled the fabrication of several meter long conductive yarns with minimal variation in the electrical resistance over the entire length of the yarn. In Figure 1i and Figure S4 (Supporting Information), we confirmed the uniform coverage of GelMA/DNA-coated MWCNT inks onto the surface of single strand cotton fibers. Furthermore, the resistance of the printed conductive inks was found to be significantly different on various substrate including PEG-coated PET films, cellulose paper, and nanofibrous electrospun sheets (Figure S5, Supporting Information). This can be due to the fact that various substrates have different roughnesses and wettability for the ink.

The applicability of the ink in the development of flexible electronics requires that the devices preserve their electrical conductivity when they are folded, bent, or stretched. To test these characteristics, an electrically conductive circuit was screen printed on a piece of cellulose paper and used to power a LED (**Figure 2**a and Figure S6, Supporting Information). The patterned circuit was connected to a power supply and was folded multiple times. The schematics in Figure 2a describe the negative and positive folding curvatures indicating folding of the printed circuit to compress or stretch the conductive layer. As shown in Figure 2a despite folding the substrate in different directions, the LED remained on and the brightness of the LED remained the same. To better characterize the foldability of the printed circuits, we measured the resistance values at different folding angles (R) and normalized them to the initial resistance (R_0) (inset of Figure 2b). In Figure 2b, we observed a 25% variation in the measured resistance under various folding angles. Also, since the ink was comprised of interconnected MWCNTs, inward (negative angles) folding compressed the CNTs and

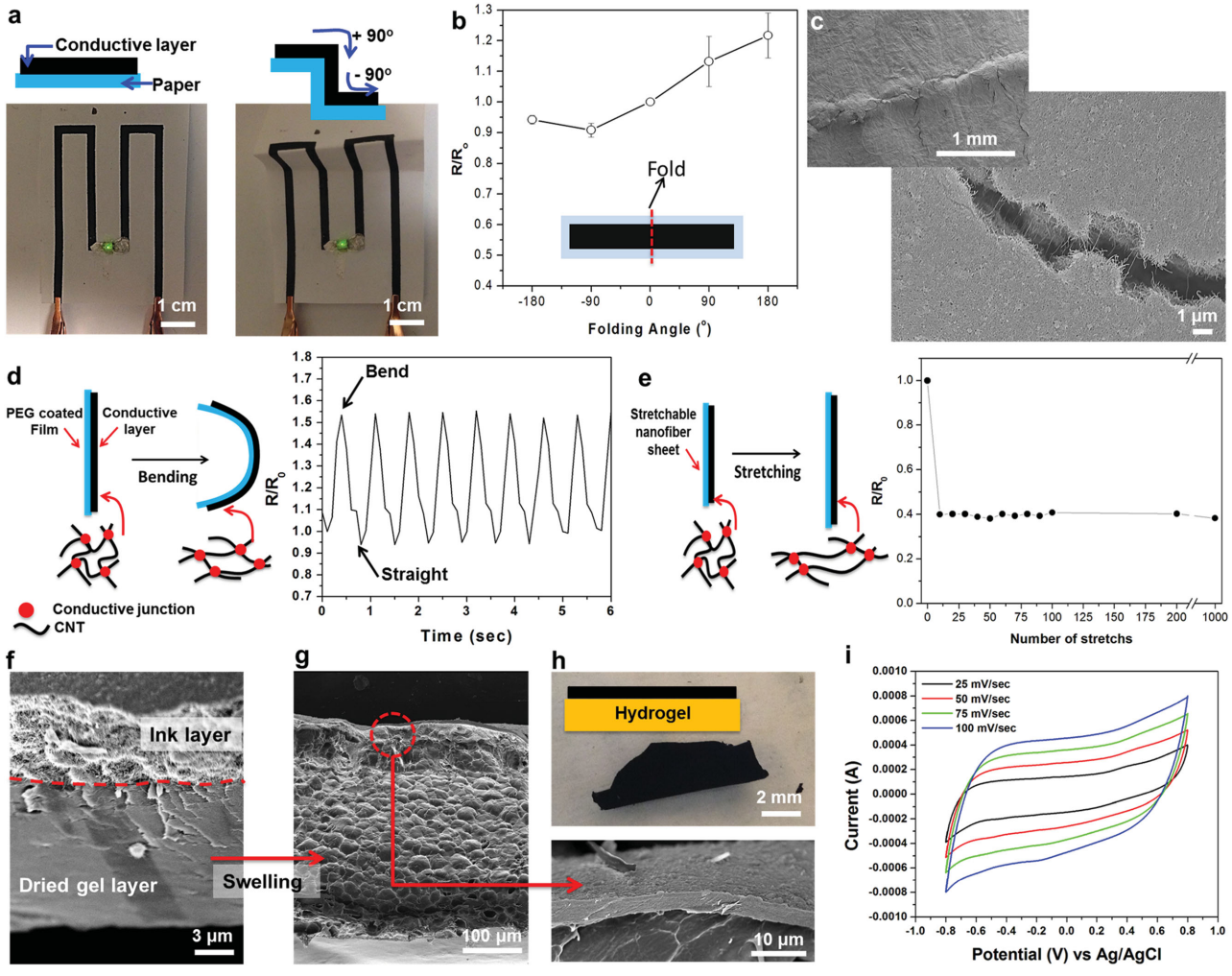

Figure 2. Electrical characteristics of printed inks on flexible substrates during deformation. a) Operation of an LED connected by ink circuits screen-printed on a cellulose paper substrate before and after folding. b) Relative resistance change of the screen-printed ink circuits fabricated on cellulose paper substrates and folded under various curvature angles. The inset is a schematic diagram of the ink circuit used for the measurement (length × width = 5 cm × 1 cm). c) SEM image of ink circuits on cellulose paper substrates after folding (180°). d) Schematic diagram and the change in relative resistance after dynamic and cyclic bending deformation of the screen printed ink circuit on a PEG-coated PET film. e) Schematic diagram and relative resistance change as a function of elongation for ink circuits on stretchable PGS/PCL substrate ($\varepsilon = 0.2$ tensile strain). f,g) Representative SEM images showing the cross-section of the ink-covered 7% GelMA hydrogel (double layer) (f) before and (g) after swelling in PBS. h) Photographs showing ink-covered GelMA hydrogels after swelling in PBS. i) Cyclic voltammetry of the ink-coated 7% GelMA hydrogel in PBS.

generated more connections, resulting in a reduction in the electrical resistance. On the other hand, when the patterns were folded outward and the ink was stretched, the connections between the CNTs loosened or some of the CNTs disconnected from each other, resulting in an increase in electrical resistance. In Figure 2c, the printed circuit after folding was imaged using an SEM, showing the interconnected nanotube network between the crack, where no obvious detachment from the substrate was observed. This result revealed that the folded circuits were capable of maintaining their conductivity.

To assess the variations in the electrical resistance of the ink during cyclic bending deformations, we dispensed the conductive ink onto a PEG-coated PET film by a screen printing process without photocrosslinking and dynamically compressed the structure up to 40% of its initial length during each cycle, as shown in Figure 2d and Figure S7 (Supporting Information). The electrical resistance was found to increase during bending deformations possibly due to the stretching of the CNT networks as shown in the schematic diagram in Figure 2d. The results showed that the variations in resistance during multiple bending cycles were about the same (≈60%) where no indication of fracture or breakage in the ink was observed. To confirm the stretchability of the electrically conductive ink, a simple conductive wire was screen printed on a piece of poly(glycerol sebacate)/poly(caprolactone) (PGS/PCL) elastomeric electrospun sheet with a paint brush.[38] As shown in Figure 2e, the resistance of the printed conductive wire on PGS/PCL substrates was measured under cyclic tensile strain ($\varepsilon = 0.2$; strain rate of 0.1 mm min^{-1}) using a two-probe measurement technique. Resistance of the conductive wire at a fixed strain value during mechanical cycling was stable, because the yielding of each fiber at a fixed strain was the same. The recorded resistance values (R) were normalized to the initial resistance R_0 of the samples at no load condition ($\varepsilon = 0$), and are shown in Figure 2e. Interestingly, the resistance was significantly decreased by 60% and stabilized after ten stretch cycles at $\varepsilon = 0.2$. After these initial variations, the resistance of the printed conductive wire on PGS/PCL remained stable and did not show any detectable drift during the next 1000 cycles. Due to the curvy architecture of the fibers within electrospun mats, stable recovery of the conductivity after the removal of the strain is possible.[15,39] In addition, the strong adhesion between the GelMA/DNA-coated MWCNTs and the electrospun substrates prevented mechanical failure (detachment of the fibers) at the interface during deformation. We also confirmed the uniform deposition of GelMA/DNA-coated MWCNT on the surface of electrospun substrates using SEM (Figure S8, Supporting Information).

Swelling, elastic properties, and electrical stability under biological conditions and on biological substrates such as hydrogels are other important parameters in the utilization of electrically conductive inks in biomedical applications. However, hydrogels have been shown to experience large volume changes while swelling in biological media. The high water content of hydrogels can induce damage or delamination of the metal electrodes deposited on the gel substrates. To assess the utilization of the ink on highly swellable hydrogel substrates, a dried 7% GelMA hydrogel substrate (thickness: ≈10 μm) was coated with the ink solution using a simple drop-casting procedure. After the drying process, a ≈3 μm thick conductive layer was formed on a ≈10 μm thick GelMA hydrogel substrate, as shown in Figure 2f. The two layers showed significantly different morphology with the well-defined MWCNT network on the top and a dense dried hydrogel layer as the bottom. We then placed the structure in biological media (1X phosphate buffered saline (PBS) solution) to assess the physical and electrical properties of the conductive ink layer under substrate swelling conditions. The changes in the thickness of the ink and the hydrogel layers were measured after swelling by using SEM images and were correlated to the degree of swelling (Figure 2f,g). The degree of swelling in the conductive layer was about ≈67% which was significantly less than the swelling of the hydrogel substrate (≈3400%). Although the hydrogel substrate swelled 50 times more than the conductive layer, the bioink layer stayed intact and no breakage was observed in the layer (Figure 2g and magnified SEM image). The conductive ink-coated GelMA hydrogel composite sheet can be easily peeled off a glass substrate after swelling, as shown in Figure 2h. Furthermore, the stability of the conductive ink after soaking in aqueous solutions was assessed on other nonswelling substrates including threads, electrospun sheets, and hydrocolloids. We did not observe any variations in electrical resistance of the coating as deposited on these substrates. Rectangular samples (15 mm × 6 mm × 0.5 mm) were used for measurement of tensile mechanical properties. Interestingly, the ink-coated GelMA hydrogels showed 100 times higher elastic modulus (626.0 ± 111.5 kPa) than a pristine GelMA hydrogel (6.7 ± 0.7 kPa) as shown in Figure S9 (Supporting Information). The enhanced mechanical stability of the ink might be due to the strong π–π and hydrophobic interactions between the GelMA/DNA chains and MWCNTs sidewalls.[27]

To assess the potential of the ink-coated hydrogels as electrochemical devices such as capacitors and biosensors, cyclic voltammetry (CV) was performed with samples swollen in biological media to confirm their electroactivity (Figure S10, Supporting Information). In Figure 2i, the CV curve showing the rectangular shape revealed that the sample had a high electrical conductivity compared with pristine GelMA hydrogel (Figure S11, Supporting Information).[27] The sample had a higher capacitance (30.48 ± 6.47 F g^{-1} in PBS and 29.4 ± 4.7 F g^{-1} in cell culture media) compared to that of single-wall carbon nanotube (SWCNT) fibers spun with ≈7 F g^{-1}. It was similar to that of typical SWCNT mats with ≈30 F g^{-1} in 2 M NaCl, which had higher salt concentrations compared with PBS (≈150 × 10^{-3} M).[40] Consequently, the GelMA/DNA binder acted as an ionic conductor to allow the electrical double layer to accumulate at the MWCNT surface. In addition, electrochemical impedance spectroscopy analysis was performed to evaluate the electrical resistance and ionic transfer characteristics of swollen GelMA/DNA-coated MWCNTs in 50 × 10^{-3} M $K_3Fe(CN)_6$ solution (Figure S12, Supporting Information). The Nyquist plot exhibited a clear semicircular feature at higher frequencies, which was associated with a process limited by electron transfer. In addition, it showed a straight line in the low frequency region, which was attributed to diffusion-limited electron transfer.[41] This observation demonstrated that the electrode made of the GelMA/DNA-coated MWCNTs after swelling has a charge transfer resistance similar to other nanoparticle based electrodes.[41] Overall, we believe that the ink's performance under physical deformation such as folding, bending, and stretching and swelling conditions

is attributed to the strong physical interactions among biomaterial-coated CNTs.[42]

A key challenge with many commercially available conductive inks is their toxicity or lack of cell binding sites, which limit their potential for monitoring cellular activity or their use in the fabrication of implantable devices. To assess the cytocompatibility and cell adhesiveness of the developed ink a MIT logo was printed on a PEG-coated PET film and subsequently seeded with cardiac fibroblasts (**Figure 3**a). The seeded cardiac cells on the printed ink showed 90% cellular viability 3 d after seeding without any significant cytotoxicity as shown in Figure S13 (Supporting Information). F-actin staining results shown in Figure 3b indicated normal cellular morphology and adherence of cells to the ink pattern only. This behavior might also be due to the presence of GelMA within the ink, which possessed functional cell binding sites even after mixing with MWCNTs which supported cellular attachment.[43] The metabolic activity of the cells measured on days 1 and 3 showed a significant increase, which is an indication of enhanced cellular activity as shown in Figure 3c.

To assess the potential application of the ink-coated hydrogels for use as electrochemical biosensors, PEG-coated PET films were covered with ink strips which were used as electrodes. The electrodes were seeded with cardiomyocytes (CMs) and a CV measurement was carried out. In Figure 3d, we observed that the CV curves obtained from cell-seeded samples were narrower and had an angle compared to the ones obtained from bare electrodes due to the cells acting as an insulator and therefore reducing the capacitance of the ink electrodes (Figure 2i).[44] We then carried out 200 charge and discharge cycles and the cellular viability was assessed using a live/dead assay. The results indicated that the GelMA/DNA-coated MWCNTs did not display cytotoxic effects on the cultured cells during the electrical measurements as shown in Figure 3e. Immunostaining against sarcomeric α-actinin and connexin-43 (Cx-43) was also carried out to evaluate the expression of biomarkers indicating normal phenotype of matured CMs. A representative micrograph shown in Figure 3f indicates the expression of these biomarkers by cells despite exposure to electrical stimulation. Furthermore, to improve the stability of the ink in biological conditions, the printed ink was crosslinked upon UV exposure and was solidified after water evaporation. The enzyme-mediated degradation test of the printed films was investigated in vitro by incubating the constructs inside

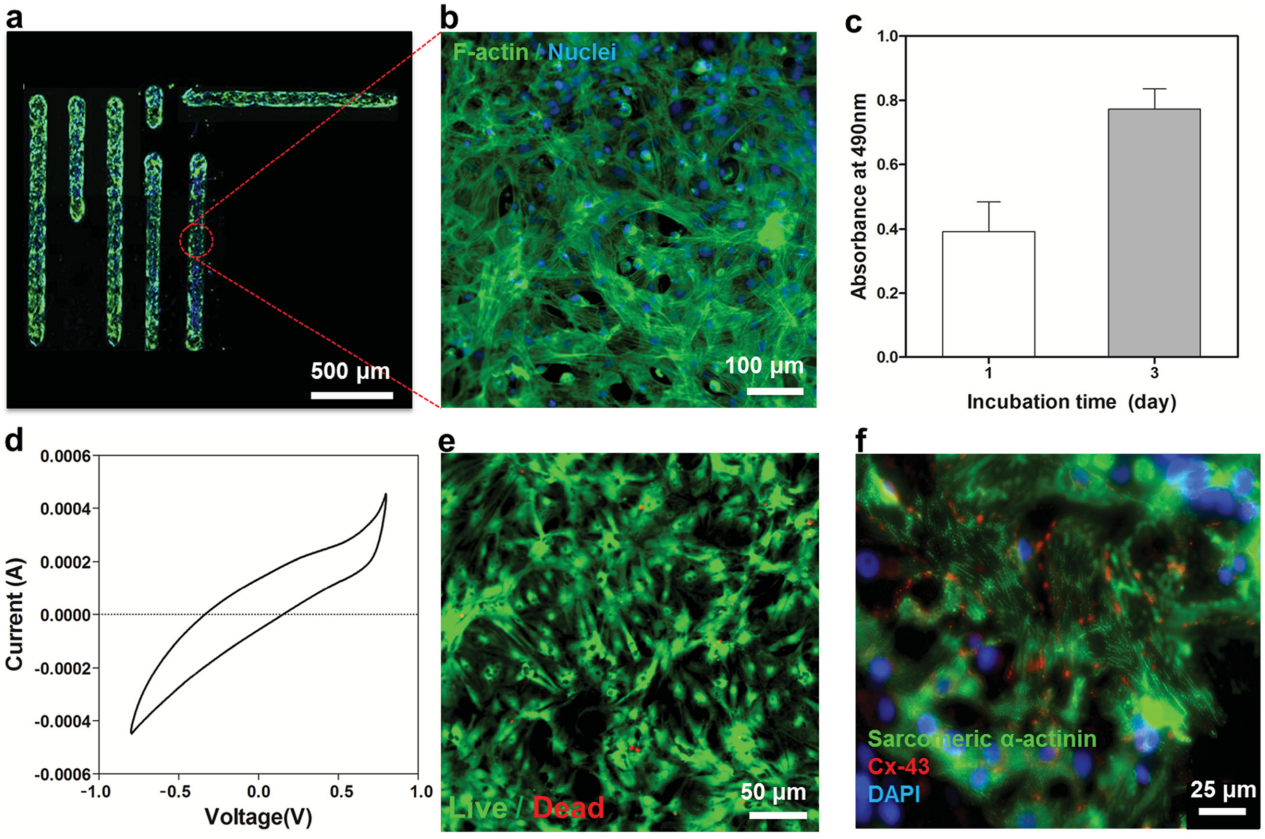

Figure 3. Cellular behavior of the engineered ink and electrical characteristics. a,b) Fluorescence images of cardiac fibroblasts cultured on ink patterns printed on PEG-coated PET film. F-actin and cell nuclei were immunostained and fluorescently labeled green and blue, respectively. c) The metabolic activity of the cells cultured on the printed ink after 1 and 3 d of culture was confirmed using the MTS (3-(4,5-dimethylthiazol-2-yl)-5-(3-carboxymethoxyphenyl)-2-(4-sulfophenyl)-2H-tetrazolium) assay. d) Cyclic voltammetry of cardiomyocytes cultured on ink electrodes fabricated on PEG-coated PET films. e) Live/dead assay after 200 charge and discharge cycles indicating high viability of cardiomyocytes. f) Immunostaining of sarcomeric α-actinin (green), cell nuclei (blue), and Cx-43 (red) revealed that the cardiac tissues (8 d culture) created on ink patterns printed on a PEG-coated PET film were phenotypically normal.

solutions containing 1 U mL^{-1} of collagenase type II. In our previous studies, the 5% GelMA hydrogels completely degraded inside solutions containing 1 U mL^{-1} of collagenase type II within 24 h.[17] However, we observed highly stable printed composite ink constructs over 5 d, possibly due to the strong binding between the CNTs and the DNA chains limiting the degradation of the ink (Figure S14, Supporting Information). Therefore, this unique property of the ink under physiological conditions will enable the creation of stable electrodes for biosensing applications.

The low viscosity of the GelMA/DNA-coated MWCNT hybrid ink was not sufficient to print the 3D constructs. To address this issue, we changed two parameters: (1) the electrostatic charge of hybrid ink and (2) the number of dispersed CNTs. Due to low negative charge density of DNA/GelMA (Figure S15, Supporting Information) resulting in weak electrostatic interactions between oppositely charged ions of GelMA/DNA and PBS, the ink did not coagulate. Therefore, DNA–CNT hybrids dispersed in GelMA could not form stable 3D constructs. To address this problem, HA was used instead of GelMA, which increased the negative charge density of the hybrid (Figure S15, Supporting Information) and thus promoted the coagulation of the bioink which encouraged 3D structure formation. In addition, the number of dispersed nanoparticles within the ink is an important parameter in viscosity of the solution and formation of mechanically strong networks. However, maximum concentration of CNTs is limited to a particular CNT mass. Therefore, the number of nanotubes in hybrid system was increased by decreasing the CNT diameter.[45] Thus, SWCNTs (diameter ≈1.2–1.7 nm) instead of MWCNTs (diameter ≈9–17 nm) was used to increase the number of CNTs in a given volume, which led to the production of 3D structures.

HA-coated SWCNTs suspension was mixed with DNA which was expected to induce instantaneous gelation after exposure to salt ions (**Figure 4**a).[46] Due to the property of DNA to coagulate under relatively low salt concentrations,[46,47] the ink solution formed microfibers in PBS. In addition, the viscosity of HA/DNA-coated SWCNT ink was relatively high compared to inkjet-printed inks. Therefore, it is expected that HA/DNA-coated SWCNT inks will be more useful for extrusion-based 3D printing approaches. Figure 4a shows the process associated with formation of microfibers and their subsequent two-step 3D printing. This coagulation process has previously been proposed in the production of polyelectrolyte microfibers.[48] The HA/DNA-coated SWCNT mixture exhibited a higher viscosity (2.05 Pa s) at 50 s^{-1} shear rate compared with GelMA/DNA-coated MWCNT ink, as shown in Figure 4b. There are two reasons for that: (1) The number of nanotubes in the ink containing the same concentration of SWCNT (diameter ≈1.2–1.7 nm) was higher than the one containing MWCNT (diameter ≈9–17 nm). (2) Higher concentration of biomaterials (10 mg mL^{-1}) for HA-based ink than GelMA-based ink (7 mg mL^{-1}) increased the viscosity of HA/DNA-coated SWCNT than that of GelMA/DNA-coated MWCNT ink. However, the HA/DNA-coated SWCNT mixture still exhibited a low viscosity compared to other CNT or graphene based inks.[32,33] The relatively low viscosity of the ink for extrusion based printing allowed the use of nozzles as small as 20 μm and increased the dispensing speed, which resulted in higher printing resolution and decreased fabrication time.[49] In addition, the shear-thinning behavior of the ink may help in preventing nozzle clogging.[50] The ink solution was aspirated into a capillary-piston (500 μm) based 3D printer and ejected into a PBS bath. The ejected inks were instantaneously coagulated resulting in microfibers. The SEM image of the printed fibers was ≈80 μm in diameter with a circular cross-section and porous surfaces (Figure 4d). The printed microfibers were deposited into 3D-defined PDMS molds using an extrusion-based bioprinter.

The generated fibers possessed superior mechanical properties with an elastic modulus of 63.56 ± 21.79 MPa and a toughness of 17.55 ± 7.14 MJ m^{-3}, as shown in Figure 4e. They were also able to withstand an elongation up to 115.33% ± 18.58%, which was similar to annealed PVA/SWCNT fibers (≈100%)[51] and was significantly higher than chitosan/SWCNT, HA/SWCNT, or DNA/SWCNT fibers (≈3%).[27] Due to the presence of HA in the ink, the dispersion of the SWCNTs in the ink remained stable throughout the process. It is also noteworthy to mention that the high surface area of the SWCNTs enabled them to interact simultaneously with both HA and DNA chains, thereby forming stable printed fibers.[18,52] The flexibility of these fibers also allowed fiber retraction into the capillary-based nozzle system and facilitated their printability.

The electrical conductivity of the fibers (including 0.3% SWCNT and 0.5% HA/DNA) was measured, using a four-point probe, to be 128 ± 15 S cm^{-1}, which was much higher than chitosan/SWCNT (2 ± 0.02 S cm^{-1}, 0.3% SWCNT),[18] graphene (53 S cm^{-1}),[53] and DNA/SWCNT (30 ± 4 S cm^{-1}, 0.4% SWCNT) fibers.[27] We measured the electrochemical activity of swollen fibers in biological media (PBS) with a 60% swelling ratio (Figure S16, Supporting Information) by CV and electrical impedance spectroscopy. In Figure 4f, the CV curves displayed a rectangular shape which was due to the electrical double layer capacitance between the HA/DNA-coated SWCNTs and the electrolyte interface. The measured electrochemical capacitance (22.81 ± 1.5 F g^{-1} in PBS solution) was higher than those from previously reported CNT/polymer composite fibers.[18] We observed lower impedance values for the fibers in PBS at high frequencies due to capacitive currents. However, the impedance of the fiber at high frequencies was found to be four times lower than the ones measured in PBS at lower frequencies (Figure 4g). In these results, the DNA and HA biocompatible binders are an excellent ion conductor similar to GelMA/DNA. Therefore, we anticipate that HA/DNA-coated SWCNT fibers have higher electrical conductivity and stronger mechanical properties compared to previously reported CNT-based materials.

Next, we integrated the 3D printed conductive fiber networks in a cardiac tissue construct. One of the ultimate goals of the project is monitoring the electrophysiological signals and promoting/regulating the electrophysiological functions of artificial cardiac and neural tissues, especially by mimicking the structures like the Purkinje fibers of the heart, where the fibers could be used as a feedback system in engineered tissues. The fibers were laid down into a 3D-defined PDMS mold using an extrusion-based bioprinter (Figure 4h). The conductive networks were surrounded with GelMA prepolymer solution mixed with cardiac cells and subsequently the prepolymer solution was crosslinked by exposure to UV light. We clearly

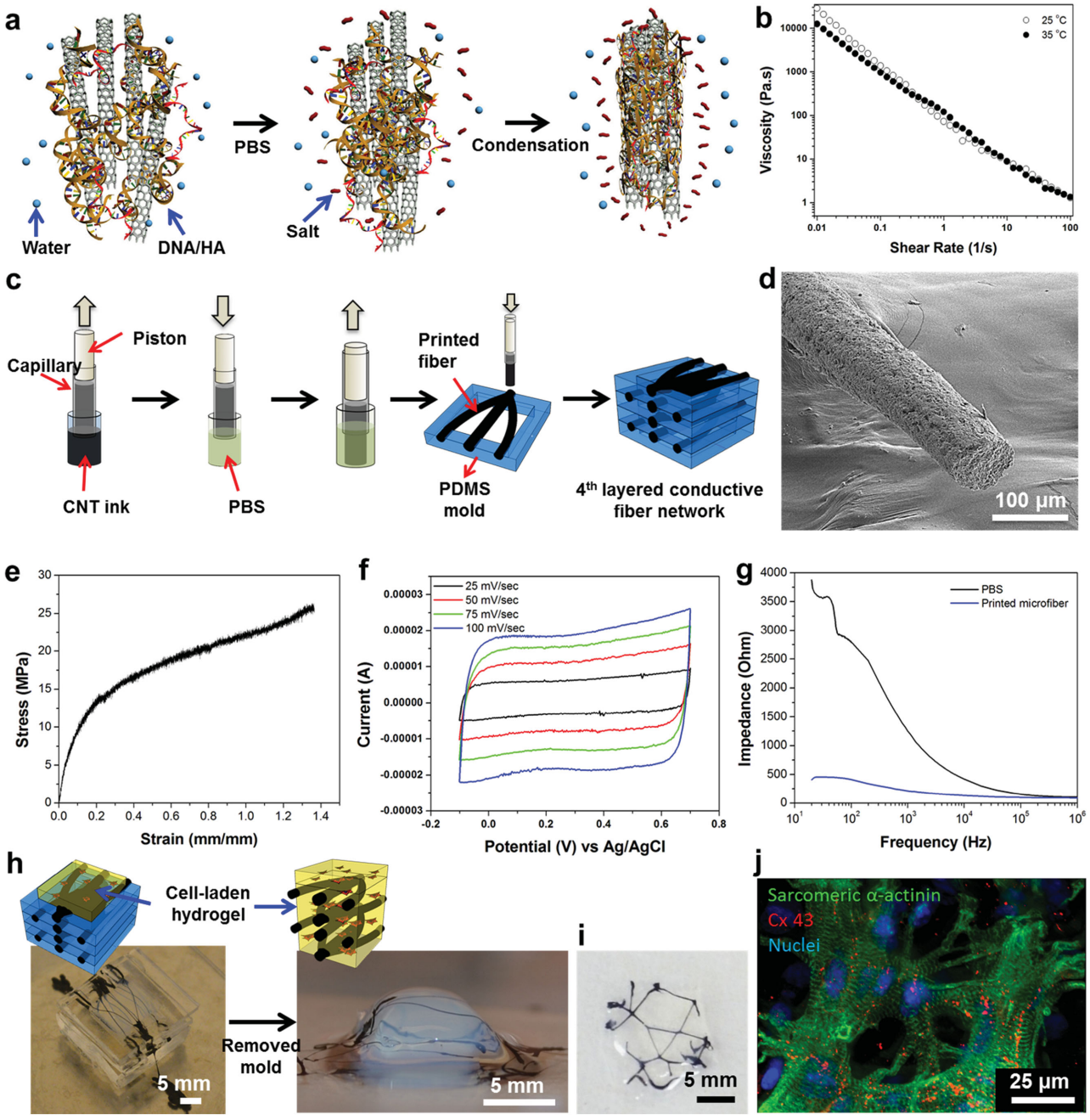

Figure 4. Ink generation and deposition process for printing 3D electrically conductive constructs. a) Schematic diagram of coagulation process of DNA/HA-coated SWCNT inks. b) Viscosity dependence as a function of shear rate for DNA/HA-coated SWCNT inks. c) Schematic diagram of the 3D printing process. d) SEM image of the porous printed fibers. e) Strain–stress curve of swollen printed fibers (elastic modulus: 63.56 ± 21.79 MPa; toughness: 17.55 ± 7.14 MJ m^{-3}; elongation: 115.33% ± 18.58%; electrical conductivity: 128 ± 15 S cm^{-1}. f) CV curves in PBS (capacitance: 22.81 ± 1.5 F g^{-1}). g) Overall impedance of printed microfibers in PBS. h) Schematic diagram showing the incorporation of a printed fiber network inside GelMA hydrogels. i) Top view of printed fiber incorporated GelMA hydrogels. j) Encapsulated cardiomyocytes in GelMA hydrogels with 3D stacked CNT fibers on day 10 immunostained for sarcomeric α-actinin (green), cell nuclei (blue), and Cx-43 (red).

observed printed fiber networks within hydrogels without any damage after the photocrosslinking step (Figure 4h,i). In addition, the encapsulated cardiac cells inside the conductive networks incorporated hydrogel expressed high degrees of maturation as evidenced by the sarcomeric α-actinin, Cx-43, and Troponin I staining (Figure 4j and Figure S17, Supporting Information). The HA/DNA-coated SWCNTs did not appear to be cytotoxic to the cells over an extended period of culture (10 d). Moreover, the incorporated fibers remained attached to the engineered constructs and showed no signs of disintegration over the culture period, emphasizing the durability of the engineered 3D electrodes.

In conclusion, we have successfully developed electrically conductive CNT-based inks that were cytocompatible. We used bio-surfactants including DNA, HA, and chemically modified gelatin to successfully improve CNT dispersion in water and its stability. In addition, the developed ink was found to be stable in aqueous solutions and biological fluids. The ink was shown to be compatible with conventional printing, dip-coating, and screen printing processes. We also demonstrated 2D and two-step 3D printing ability, which potentially allows for easy fabrication of patterned conductive structures without harsh processing conditions on various flexible substrates such as paper, hydrogels, and elastomers, while maintaining high electrical conductivity and capacitance in biological conditions. We have successfully developed foldable, bendable, and stretchable 2D electronic circuits by using a commercial printer. The developed electronic circuits displayed a small change in resistance under different folding angles and maintained their electrical connectivity after repetitive folding and unfolding cycles. The majority of the seeded cells on the printed ink were highly viable and showed good cellular behavior. In addition, the developed bioink was utilized to create 3D circuits that were embedded within hydrogel constructs. Furthermore, these printed fibers had suitable mechanical strength and high electrical conductivity suitable for various other applications. We have successfully incorporated conductive networks into cell-laden soft hydrogels without any damage or degradation in their properties. We believe that the developed CNT hybrid materials will be beneficial for fabrication of flexible and foldable biosensors and advanced functionalized tissue-engineered scaffolds.

Supporting Information

Supporting Information is available from the Wiley Online Library or from the author.

Acknowledgements

S.R.S., R.F., and A.T. contributed equally to this work. The authors declare no conflict of interests in this work. This work was supported by the National Science Foundation (EFRI-1240443), the Office of Naval Research Young Investigator Award, ONR PECASE Award, and the National Institutes of Health (HL092836, DE019024, EB012597, AR057837, DE021468, HL099073, EB008392). The project was funded by the Deanship of Scientific Research (DSR), King Abdulaziz University, under Grant No. 18-130-1434-HiCi. The authors, therefore, acknowledge with thanks DSR technical and financial support. The authors would like to thank Prof. Bradley Olsen at MIT for viscosity measurements of the ink.

Received: December 27, 2015
Published online: February 24, 2016

[1] a) A. M. Gaikwad, G. L. Whiting, D. A. Steingart, A. C. Arias, *Adv. Mater.* **2011**, *23*, 3251; b) D.-H. Kim, N. Lu, R. Ghaffari, J. A. Rogers, *NPG Asia Mater.* **2012**, *4*, 15; c) F. Garnier, R. Hajlaoui, A. Yassar, P. Srivastava, *Science* **1994**, *265*, 1684; d) X. Duan, T. M. Fu, J. Liu, C. M. Lieber, *Nano Today* **2013**, *8*, 351.

[2] a) N. Lu, D.-H. Kim, *Soft Robotics* **2014**, *1*, 9; b) G. S. Jeong, D. H. Baek, H. C. Jung, J. H. Song, J. H. Moon, S. W. Hong, I. Y. Kim, S. H. Lee, *Nat. Commun.* **2012**, *3*, 977.

[3] S. Jung, J. H. Kim, J. Kim, S. Choi, J. Lee, I. Park, T. Hyeon, D. H. Kim, *Adv. Mater.* **2014**, *26*, 4825.

[4] D. H. Kim, N. Lu, R. Ma, Y. S. Kim, R. H. Kim, S. Wang, J. Wu, S. M. Won, H. Tao, A. Islam, K. J. Yu, T. I. Kim, R. Chowdhury, M. Ying, L. Xu, M. Li, H. J. Chung, H. Keum, M. McCormick, P. Liu, Y. W. Zhang, F. G. Omenetto, Y. Huang, T. Coleman, J. A. Rogers, *Science* **2011**, *333*, 838.

[5] T. Cheng, Y. Zhang, W. Y. Lai, W. Huang, *Adv. Mater.* **2015**, *27*, 3349.

[6] R. C. Webb, A. P. Bonifas, A. Behnaz, Y. Zhang, K. J. Yu, H. Cheng, M. Shi, Z. Bian, Z. Liu, Y. S. Kim, W. H. Yeo, J. S. Park, J. Song, Y. Li, Y. Huang, A. M. Gorbach, J. A. Rogers, *Nat. Mater.* **2013**, *12*, 938.

[7] a) D. Son, J. Lee, S. Qiao, R. Ghaffari, J. Kim, J. E. Lee, C. Song, S. J. Kim, D. J. Lee, S. W. Jun, S. Yang, M. Park, J. Shin, K. Do, M. Lee, K. Kang, C. S. Hwang, N. Lu, T. Hyeon, D. H. Kim, *Nat. Nanotechnol.* **2014**, *9*, 397; b) A. H. Najafabadi, A. Tamayol, N. Annabi, M. Ochoa, P. Mostafalu, M. Akbari, M. Nikkhah, R. Rahimi, M. R. Dokmeci, S. Sonkusale, B. Ziaie, A. Khademhosseini, *Adv. Mater.* **2014**, *26*, 5823.

[8] a) J. Zang, S. Ryu, N. Pugno, Q. Wang, Q. Tu, M. J. Buehler, X. Zhao, *Nat. Mater.* **2013**, *12*, 321; b) C. F. Guo, T. Sun, Q. Liu, Z. Suo, Z. Ren, *Nat. Commun.* **2014**, *5*, 3121; c) W. Deng, X. Zhang, H. Pan, Q. Shang, J. Wang, J. Jie, *Sci. Rep.* **2014**, *4*, 5358.

[9] E. B. Secor, P. L. Prabhumirashi, K. Puntambekar, M. L. Geier, M. C. Hersam, *J. Phys. Chem. Lett.* **2013**, *4*, 1347.

[10] J. T. Muth, D. M. Vogt, R. L. Truby, Y. Menguc, D. B. Kolesky, R. J. Wood, J. A. Lewis, *Adv. Mater.* **2014**, *26*, 6307.

[11] E. B. Secor, S. Lim, H. Zhang, C. D. Frisbie, L. F. Francis, M. C. Hersam, *Adv. Mater.* **2014**, *26*, 4533.

[12] A. E. Jakus, E. B. Secor, A. L. Rutz, S. W. Jordan, M. C. Hersam, R. N. Shah, *ACS Nano* **2015**, *9*, 4636.

[13] K. Sun, T. S. Wei, B. Y. Ahn, J. Y. Seo, S. J. Dillon, J. A. Lewis, *Adv. Mater.* **2013**, *25*, 4539.

[14] H. L. Hsu, I. J. Teng, Y. C. Chen, W. L. Hsu, Y. T. Lee, S. J. Yen, H. C. Su, S. R. Yeh, H. Chen, T. R. Yew, *Adv. Mater.* **2010**, *22*, 2177.

[15] K. Y. Chun, Y. Oh, J. Rho, J. H. Ahn, Y. J. Kim, H. R. Choi, S. Baik, *Nat. Nanotechnol.* **2010**, *5*, 853.

[16] a) K. Kordas, T. Mustonen, G. Toth, H. Jantunen, M. Lajunen, C. Soldano, S. Talapatra, S. Kar, R. Vajtai, P. M. Ajayan, *Small* **2006**, *2*, 1021; b) H. Koo, W. Lee, Y. Choi, J. Sun, J. Bak, J. Noh, V. Subramanian, Y. Azuma, Y. Majima, G. Cho, *Sci. Rep.* **2015**, *5*, 14459; c) H. Okimoto, T. Takenobu, K. Yanagi, Y. Miyata, H. Shimotani, H. Kataura, Y. Iwasa, *Adv. Mater.* **2010**, *22*, 3981.

[17] S. R. Shin, H. Bae, J. M. Cha, J. Y. Mun, Y.-C. Chen, H. Tekin, H. Shin, S. Farshchi, M. R. Dokmeci, X. Tang, A. Khademhosseini, *ACS Nano* **2012**, *6*, 362.

[18] C. Lynam, S. E. Moulton, G. G. Wallace, *Adv. Mater.* **2007**, *19*, 5.

[19] J. V. Veetil, K. Ye, *Biotechnol. Prog.* **2009**, *25*, 709.

[20] X. Xiong, C. L. Chen, P. Ryan, A. A. Busnaina, Y. J. Jung, M. R. Dokmeci, *Nanotechnology* **2009**, *20*, 295302.

[21] J. W. Nichol, S. T. Koshy, H. Bae, C. M. Hwang, S. Yamanlar, A. Khademhosseini, *Biomaterials* **2010**, *31*, 5536.

[22] S. Giraudier, D. Hellio, M. Djabourov, V. Larreta-Garde, *Biomacromolecules* **2004**, *5*, 1662.

[23] S. R. Shin, S. M. Jung, M. Zalabany, K. Kim, P. Zorlutuna, S. B. Kim, M. Nikkhah, M. Khabiry, M. Azize, J. Kong, K. T. Wan, T. Palacios, M. R. Dokmeci, H. Bae, X. S. Tang, A. Khademhosseini, *ACS Nano* **2013**, *7*, 2369.

[24] S. S. Karajanagi, H. Yang, P. Asuri, E. Sellitto, J. S. Dordick, R. S. Kane, *Langmuir* **2006**, *22*, 1392.

[25] Y. Liu, X. Liu, X. Wang, *Nanoscale Res. Lett.* **2011**, *6*, 22.

[26] Z. Zhou, H. Kang, M. L. Clarke, S. H. Lacerda, M. Zhao, J. A. Fagan, A. Shapiro, T. Nguyen, J. Hwang, *Small* **2009**, *5*, 2149.
[27] S. R. Shin, C. K. Lee, I. So, J. H. Jeon, T. M. Kang, C. Kee, S. I. Kim, G. M. Spinks, G. G. Wallace, S. K. Kim, *Adv. Mater.* **2008**, *20*, 5.
[28] M. Hughes, G. M. Spinks, *Adv. Mater.* **2005**, *17*, 4.
[29] W. Huang, S. Taylor, K. Fu, D. Zhang, T. W. Hanks, A. M. Rao, Y.-P. Sun, *Nano Lett.* **2002**, *2*, 311.
[30] F. Torrisi, T. Hasan, W. Wu, Z. Sun, A. Lombardo, T. S. Kulmala, G.-W. Hsieh, S. Jung, F. Bonaccorso, P. J. Paul, D. Chu, A. C. Ferrari, *ACS Nano* **2012**, *6*, 2992.
[31] B. S. Shim, W. Chen, C. Doty, C. Xu, N. A. Kotov, *Nano Lett.* **2008**, *8*, 4151.
[32] E. Garcia-Tunon, S. Barg, J. Franco, R. Bell, S. Eslava, E. D'Elia, R. C. Maher, F. Guitian, E. Saiz, *Adv. Mater.* **2015**, *27*, 1688.
[33] B. G. Compton, J. A. Lewis, *Adv. Mater.* **2014**, *26*, 5930.
[34] a) H. Onoe, T. Okitsu, A. Itou, M. Kato-Negishi, R. Gojo, D. Kiriya, K. Sato, S. Miura, S. Iwanaga, K. Kuribayashi-Shigetomi, *Nat. Mater.* **2013**, *12*, 584; b) E. Brouzes, M. Medkova, N. Savenelli, D. Marran, M. Twardowski, J. B. Hutchison, J. M. Rothberg, D. R. Link, N. Perrimon, M. L. Samuels, *Proc. Natl. Acad. Sci. USA* **2009**, *106*, 14195; c) M. Yamada, R. Utoh, K. Ohashi, K. Tatsumi, M. Yamato, T. Okano, M. Seki, *Biomaterials* **2012**, *33*, 8304.
[35] W. J. Hyun, S. Lim, B. Y. Ahn, J. A. Lewis, C. D. Frisbie, L. F. Francis, *ACS Appl. Mater. Interfaces* **2015**, *7*, 12619.
[36] M. D. Lima, N. Li, M. Jung de Andrade, S. Fang, J. Oh, G. M. Spinks, M. E. Kozlov, C. S. Haines, D. Suh, J. Foroughi, S. J. Kim, Y. Chen, T. Ware, M. K. Shin, L. D. Machado, A. F. Fonseca, J. D. Madden, W. E. Voit, D. S. Galvao, R. H. Baughman, *Science* **2012**, *338*, 928.
[37] M. Akbari, A. Tamayol, V. Laforte, N. Annabi, A. H. Najafabadi, A. Khademhosseini, D. Juncker, *Adv. Funct. Mater.* **2014**, *24*, 4060.
[38] a) M. Kharaziha, M. Nikkhah, S. R. Shin, N. Annabi, N. Masoumi, A. K. Gaharwar, G. Camci-Unal, A. Khademhosseini, *Biomaterials* **2013**, *34*, 6355; b) M. Kharaziha, S. R. Shin, M. Nikkhah, S. N. Topkaya, N. Masoumi, N. Annabi, M. R. Dokmeci, A. Khademhosseini, *Biomaterials* **2014**, *35*, 7346.
[39] M. Park, J. Im, M. Shin, Y. Min, J. Park, H. Cho, S. Park, M. B. Shim, S. Jeon, D. Y. Chung, J. Bae, U. Jeong, K. Kim, *Nat. Nanotechnol.* **2012**, *7*, 803.
[40] a) M. E. Kozlov, R. C. Capps, W. M. Sampson, V. H. Ebron, J. P. Ferraris, R. H. Baughman, *Adv. Mater.* **2005**, *17*, 4; b) J. N. Barisci, M. Tahhan, G. G. Wallace, S. Badaire, T. Vaugien, M. Maugey, P. Poulin, *Adv. Mater.* **2004**, *14*, 6.
[41] Q. Liu, Q. Shi, H. WAng, Q. Zhang, Y. Li, *RSC Adv.* **2015**, *5*, 6.
[42] A. N. Volkov, L. V. Zhigilei, *ACS Nano* **2010**, *4*, 6187.
[43] a) M. Abdul Kafi, W. A. El-Said, T. H. Kim, J. W. Choi, *Biomaterials* **2011**, *33*, 731; b) K. Y. Baik, S. Y. Park, K. Heo, K. B. Lee, S. Hong, *Small* **2011**, *7*, 741; c) S. Namgung, T. Kim, K. Y. Baik, M. Lee, J. M. Nam, S. Hong, *Small* **2011**, *7*, 56.
[44] A. Venkatanarayanan, T. E. Keyes, R. J. Forster, *Anal. Chem.* **2013**, *85*, 2216.
[45] A. Szabo, C. Perri, A. Csato, G. Giordano, D. Vuono, J. B. Nagy, *Mater. Today* **2010**, *3*, 38.
[46] C. K. Lee, S. R. Shin, J. Y. Mun, S. S. Han, I. So, J. H. Jeon, T. M. Kang, S. I. Kim, P. G. Whitten, G. G. Wallace, G. M. Spinks, S. J. Kim, *Angew. Chem. Int. Ed.* **2009**, *48*, 5116.
[47] C. K. Lee, S. R. Shin, S. H. Lee, J. H. Jeon, I. So, T. M. Kang, S. I. Kim, J. Y. Mun, S. S. Han, G. M. Spinks, G. G. Wallace, S. J. Kim, *Angew. Chem. Int. Ed.* **2008**, *47*, 2470.
[48] a) H. P. Cong, X. C. Ren, P. Wang, S. H. Yu, *Sci. Rep.* **2012**, *2*, 613; b) A. Tamayol, M. Akbari, N. Annabi, A. Paul, A. Khademhosseini, D. Juncker, *Biotechnol. Adv.* **2013**, *31*, 669.
[49] T. Jungst, W. Smolan, K. Schacht, T. Scheibel, J. Groll, *Chem. Rev.* **2015**, DOI:10.1021/acs.chemrev.5b00303.
[50] C. Zhu, T. Y. Han, E. B. Duoss, A. M. Golobic, J. D. Kuntz, C. M. Spadaccini, M. A. Worsley, *Nat. Commun.* **2015**, *6*, 6962.
[51] M. K. Shin, B. Lee, S. H. Kim, J. A. Lee, G. M. Spinks, S. Gambhir, G. G. Wallace, M. E. Kozlov, R. H. Baughman, S. J. Kim, *Nat. Commun.* **2012**, *3*, 650.
[52] a) J. F. Campbell, M. E. Napier, S. W. Feldberg, H. H. Thorp, *J. Phys. Chem. B* **2010**, *114*, 8861; b) M. Zheng, A. Jagota, E. D. Semke, B. A. Diner, R. S. McLean, S. R. Lustig, R. E. Richardson, N. G. Tassi, *Nat. Mater.* **2003**, *2*, 338; c) C. Zamora-Ledezma, L. Buisson, S. E. Moulton, G. Wallace, C. Zakri, C. Blanc, E. Anglaret, P. Poulin, *Langmuir* **2013**, *29*, 10247.
[53] X. Zhen, G. Chao, *Mater. Today* **2015**, *18*, 12.